ELSEVIER

Chemistry & Biology 8 (2001) 1025–1032

Chemistry & Biology

www.elsevier.com/locate/chembiol

Research Paper

De novo design of fibrils made of short α-helical coiled coil peptides

S.A. Potekhin [a], T.N. Melnik [a], V. Popov [b], N.F. Lanina [c], A.A. Vazina [c], P. Rigler [d], A.S. Verdini [e], G. Corradin [f], A.V. Kajava [g,*]

[a] *Institute of Protein Research, Russian Academy of Science, 142292 Pushchino, Moscow Region, Russia*
[b] *Institute of Cell Biophysics, Russian Academy of Science, 142292 Pushchino, Moscow Region, Russia*
[c] *Institute of Theoretical and Experimental Biophysics, Russian Academy of Science, 142292 Pushchino, Moscow Region, Russia*
[d] *Institute of Physical Chemistry, EPFL, CH-1015 Lausanne-Ecublens, Switzerland*
[e] *Dictagene, Ch. des Boveresses 155, CH-1066 Epalinges, Switzerland*
[f] *Institute of Biochemistry, University of Lausanne, Ch. des Boveresses 155, CH-1066 Epalinges, Switzerland*
[g] *Swiss Institute for Experimental Cancer Research, Ch. des Boveresses 155, CH-1066 Epalinges, Switzerland*

Received 5 April 2001; revisions requested 31 May 2001; revisions received 25 June 2001; accepted 2 July 2001
First published online 12 September 2001

Abstract

Background: The α-helical coiled coil structures formed by 25–50 residues long peptides are recognized as one of Nature's favorite ways of creating an oligomerization motif. Known de novo designed and natural coiled coils use the lateral dimension for oligomerization but not the axial one. Previous attempts to design α-helical peptides with a potential for axial growth led to fibrous aggregates which have an unexpectedly big and irregular thickness. These facts encouraged us to design a coiled coil peptide which self-assembles into soluble oligomers with a fixed lateral dimension and whose α-helices associate in a staggered manner and trigger axial growth of the coiled coil. Designing the coiled coil with a large number of subunits, we also pursue the practical goal of obtaining a valuable scaffold for the construction of multivalent fusion proteins.

Results: The designed 34-residue peptide self-assembles into long fibrils at slightly acid pH and into spherical aggregates at neutral pH. The fibrillogenesis is completely reversible upon pH change. The fibrils were characterized using circular dichroism spectroscopy, sedimentation diffusion, electron microscopy, differential scanning calorimetry and X-ray fiber diffraction. The peptide was deliberately engineered to adopt the structure of a five-stranded coiled coil rope with adjacent α-helices, staggered along the fibril axis. As shown experimentally, the most likely structure matches the predicted five-stranded arrangement.

Conclusions: The fact that the peptide assembles in an expected fibril arrangement demonstrates the credibility of our conception of design. The discovery of a short peptide with fibril-forming ability and stimulus-sensitive behavior opens new opportunities for a number of applications.

Keywords: Coiled coil; Design; Fibril; Peptide synthesis; Stimulus-sensitive hydrogel

1. Introduction

One of the main goals of chemistry is to achieve control over the structure of synthetic molecules, opening the way for new applications, ranging from materials science to medicine. Obtaining de novo designed molecules with a priori predicted properties is a convincing proof of success in this direction. Although, in general, the design of protein structures is still a risky task frequently resulting in failure to obtain a desired structure, several successful attempts to design α-helical coiled coil structures have been reported [1,2]. The designed coiled coils included dimers, trimers and tetramers, oriented parallel and antiparallel, forming homo- and hetero-oligomers, structures with left- and right-hand superhelical twists [1–3]. However, all these structures as well as all known natural coiled coils [3,4] are compact α-helical bundles which do not use the axial direction for oligomerization. Previous attempts to design α-helical coiled coils with ability to grow in the axial direction resulted in fibrous aggregates of irregular

Abbreviations: CD, circular dichroism; αFFP, α-helical fibril-forming peptide

* Corresponding author. Present address: Center for Molecular Modeling, CIT, National Institutes of Health, Bldg. 12A, Bethesda, MD 20892-5626, USA.
E-mail address: kajava@helix.nih.gov (A.V. Kajava).

1074-5521/01/$ – see front matter
PII: S1074-5521(01)00073-4

thickness that was an order of magnitude greater than anticipated for the designed coiled coils [5,6]. We describe here a design of a peptide forming soluble fibrils of defined diameter. The novel coiled coil architecture was achieved by imparting to the short α-helices a potential for lateral pentamerization and axial staggering. Designing an oligomer with a large number of subunits, we also had in mind the practical goal of creating a valuable scaffold for the construction of multivalent fusion proteins, knowing that for this purpose the coiled coil with the highest number of subunits is especially promising [7].

2. Results

2.1. Design of α-helical fibril-forming peptide

The α-helical coiled coil structures share a seven-residue repeat $(\mathbf{abcdefg})_n$ containing hydrophobic residues at positions **a** and **d** and polar residues generally elsewhere. Our design was based on the assumption that the peptide length and repetition of identical heptads are important factors to promote fibrillar association. Indeed, the identical repeats build in a possibility for the helices to be axially staggered because such α-helices being shifted by multiples of the heptad have almost the same interhelical interactions in the parallel (in terms of the peptide N–C direction) coiled coils. The staggering could open a new dimension of the coiled coil propagation and trigger an unprecedentedly high multimeric associate. As concerns the peptide length (L), the shifts Δl of the adjacent α-helices should be equal to a value divisible by one heptad (Fig. 1a). On the other hand, the staggered helices of the n-stranded rope complete one turn without overlapping of the i-th and $(i+n)$-th α-helices, if the shift is more than $(L+\delta l)/n$, where δl is an addition, equal to one residue, to give a space for head-to-tail packing of α-helices. The shift of more than $(L+\delta l)/n$ may also be unfavorable because it leads to the head-to-tail gap and exposure of some **a** and **d** residues to the solvent. Thus, in accordance with this consideration, the most favorable minimal length of the α-helix for an n-stranded rope is $(n\times 7-1)$ residues, i.e. 20, 27 and 34 residues for the three-, four- and five-stranded fibrils, respectively.

Assuming that the longer the peptide the higher its ability to oligomerize, we chose a 34 residues long peptide and focused on the design of a five-stranded structure similar to the most recently identified five-stranded α-helical bundles [8,10,11]. Establishment of interactions, which control the number of strands in the coiled coils, presents another major challenge. It is known that fragments in a range of 20–50 residues with the common coiled coil pattern form two-, three-, four- and even five-stranded helical bundles depending on slight variations in their sequences [8,12–15]. Despite some progress [12–15], the rules governing the stoichiometry of the coiled coils are largely unknown

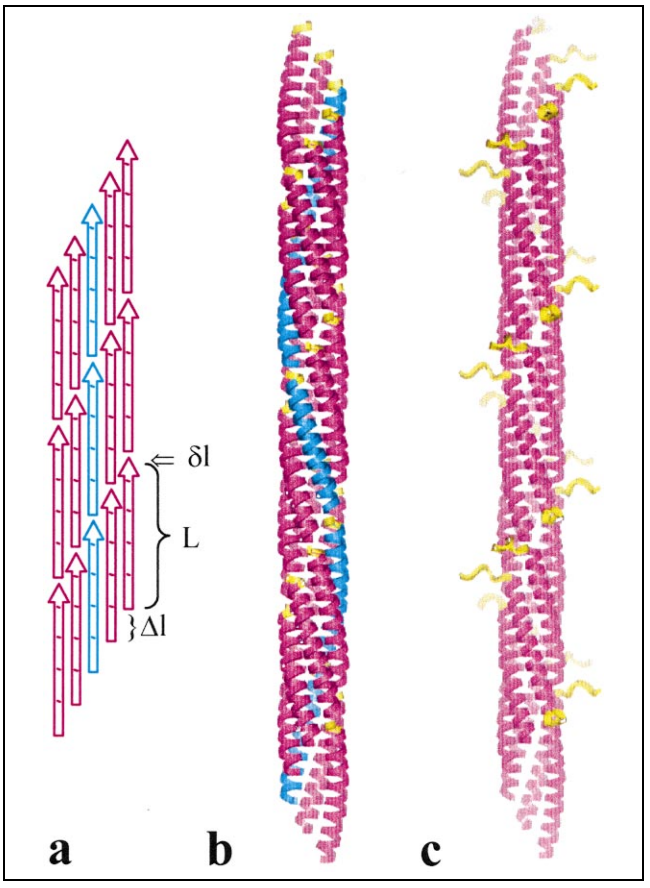

Fig. 1. (a) Two-dimensional schematic representation of a five-stranded fibril with staggered α-helices. α-Helices are shown as arrows with cross-lines indicating the heptad repeats. (b) Structural model of α-helical five-stranded fibril containing 34-residue peptides. Each strand is formed by the α-helices aligned head-to-tail (one strand is shown in blue, N-termini are in yellow). The strands are wrapped around the coiled coil axis in a left-handed superhelix with parameters similar to the ones of the known pentameric coiled coil [8]. The equivalent positions of the adjacent α-helices trace out a right-handed helical trajectory. (c) Model of the fibril built of peptides with five additional residues (in yellow) of non-coiled coil sequence. The structures were modeled and the picture was generated by the Insight II package [9]. The atomic coordinates are available on the World Wide Web (http://cmm.info.nih.gov/kajava).

[3,4]. Analysis of the known five-stranded coiled coil structures allowed us to formulate a hypothesis which states that favorable interactions between side chains in the **b**, **c**, **e**, **f**, and **g** positions play an important and sometimes critical role in formation of the coiled coils with the highest number (four to five) of strands [11]. This hypothesis has been used to design a basic heptad repeat which was then repeated several times in the 34-residue peptide. This repetition multiplies the effect, which is supposed to force the peptide to a desirable oligomerization.

The following considerations were taken into account to design the basic heptad repeat.

1. The sequences of the known pentamers show no strong

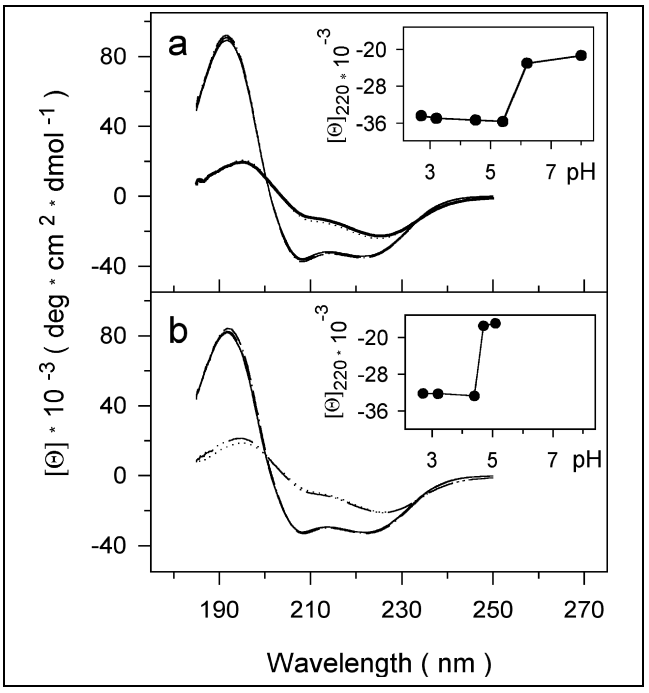

Fig. 2. Far-UV CD spectra of (a) αFFP at pH 2.7, 3.2, 4.5, 5.4, 6.2, and 8.0 and (b) QCQAC+αFFP at pH 2.7, 3.2, 4.5, 4.8, and 5.2. Spectra were recorded at a peptide concentration of 0.5 mg/ml in 10 mM sodium phosphate buffer at 20°C. Insertion shows pH dependence of $[\theta]_{220\,nm}$ values. pH values in insets are the same as in the main pictures.

bias for any particular apolar residues at either the **a** or **d** position. Therefore, in the designed peptide, positions **a** and **d** are occupied by leucine since this residue occurs most frequently in the short coiled coils.

2. Considering that apolar residues at positions **e** or **g** may cause the formation of four- or five-stranded α-coiled coils due to widening of the hydrophobic cluster [11,16–18], an alanine was placed in position **e**.
3. Glutamic acid and arginine were chosen for positions **f** and **g** because of possible interhelical **f**–**g′** electrostatic interactions in the five-stranded coiled coil [11]. Importantly, such salt bridges cannot be formed in the two- or three-stranded coiled coils. To favor the parallel orientation over the antiparallel one, the helices contain positively charged arginine on one side of the apolar interface and negatively charged glutamic acid on the other side.
4. The choice of glutamine for positions **b** and **c** was guided by the observation that, in the pentamer, they are close enough to form interhelical hydrogen bonds.

Taking into account all the constraints, the designed sequence of our α-helical fibril-forming peptide (αFFP) was $Q_cL_dA_eR_fE_gL_a(Q_bQ_cL_dA_eR_fE_gL_a)_4$.

2.2. *Experimental characterization of structures formed by αFFP*

Circular dichroism (CD) spectroscopy of the chemically synthesized αFFP shows more than 95% of the α-helical secondary structure at acid pH and room temperature (Fig. 2a). The ratio between molar ellipticities of the peptide at 220 and 208 nm is ~1.0, which has been suggested to be typical of interacting α-helices [19]. Upon pH increase, the αFFP spectrum is noticeably changed (Fig. 2a) and the peptide solution becomes slightly turbid. The transition between the dispersed and turbid states is absolutely reversible, highly cooperative and occurs at pH 5.5–6.0 (inset in Fig. 2a). Heating to 95°C at neutral pH restores the characteristic spectrum of the α-helical structure, while cooling to room temperature returns the peptide to the precipitated state.

In accordance with the sedimentation–diffusion study, the sedimentation profile of the preparation has one symmetrical peak at 5.0S, a diffusion coefficient of 1.35×10^{-7} cm^2/s at acid pH and a concentration of 1.5 mg/ml. This suggests that at acid pH, peptides assemble in elongated structures of about 80 peptide molecules and a large-to-small radius ratio of more than 20. Electron microscopy study shows that these oligomers are uniform fibrils whose diameter is about 3.2 ± 0.5 nm (Fig. 3A,B), while at neutral pH the associates are spherical particles with diameters of 10–15 nm (Fig. 3C).

Calorimetric study shows that the fibrils are extremely stable, showing no signs of denaturing up to 130°C (the limit of the instrument) in aqueous solution. Therefore, denaturing reagents such as GuHCl, dimethylsulfoxide (DMSO) and urea were added to lower the denaturing temperature. Reproducible melting curves were obtained in DMSO (Fig. 4). Although the fibrils retain an unusually high stability even in DMSO as compared with other proteins [20], they are cooperatively melted at 99°C and 120°C respectively in 75% and 60% DMSO (Table 1). As seen from Fig. 4, the melting curves are asymmetric. This is compatible with the irreversible one-stage model $A\rightarrow B$ or can be an indication of non-equilibrium processes [21]. Our experiments favor the latter explanation. Indeed, upon a repeated heating of the preparations, the main transitions of the melting curves are reproduced com-

Table 1
Melting curves parameters of the designed peptide at different DMSO concentrations[a]

	T_d (K)	ΔH_{cal} (kJ/mol)[b]	$\Delta T_{1/2}$ (K)	ΔH_{eff} (kJ/mol)	$\Delta H_{cal}/\Delta H_{eff}$
60% DMSO	393.0	179	14.7	360	2.0
75% DMSO	372.0	125	15.6	295	2.4

[a] 10 mM sodium phosphate buffer, pH 2.5. Peptide concentration is 1.2 mg/ml.
[b] ΔH_{cal} values were measured for the main peaks.

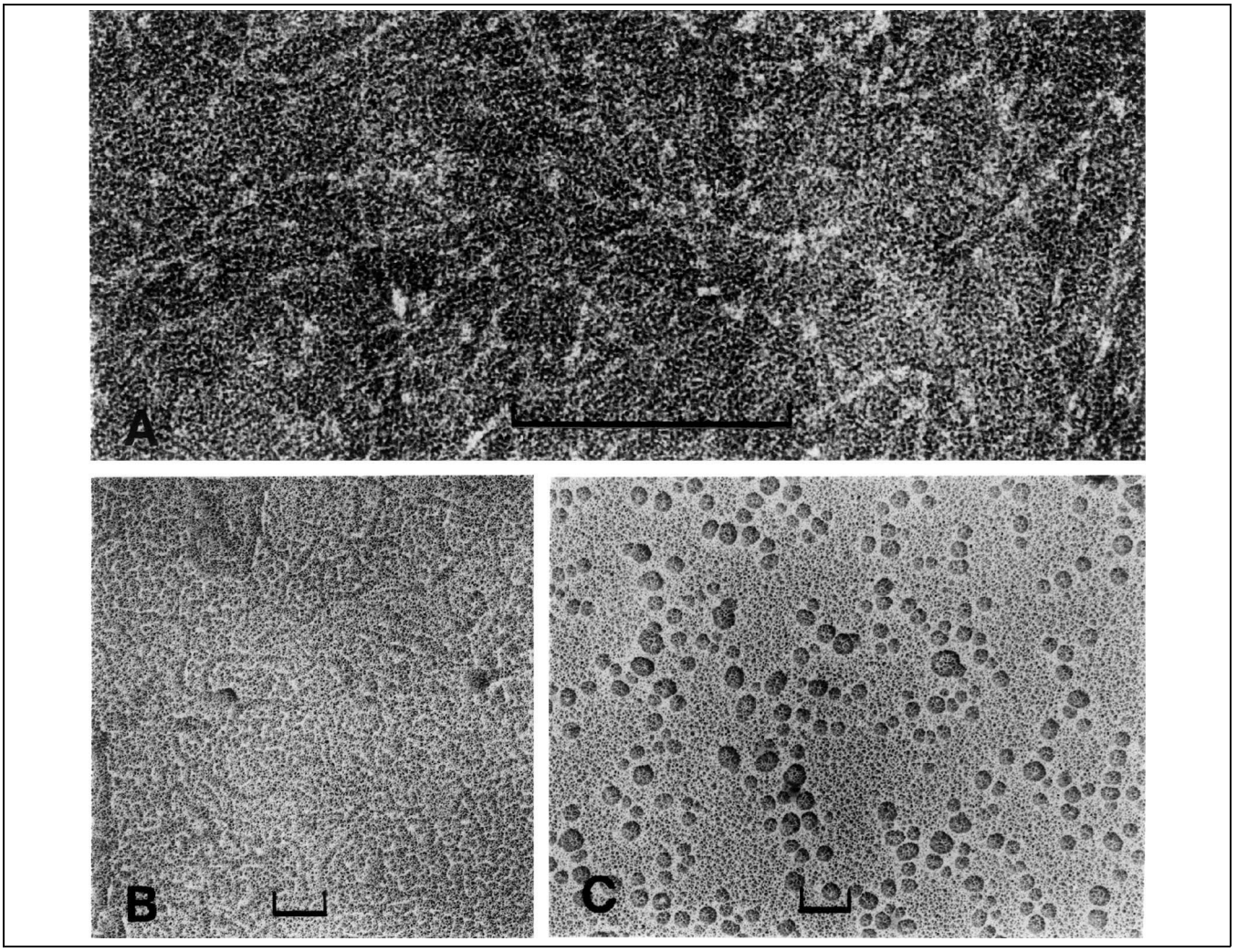

Fig. 3. Electron microscopy pictures of (A) fibrils negatively stained with uranyl acetate (pH 2.8), (B) rotary shadowed fibrils (pH 2.8) and (C) rotary shadowed spherical particles (pH 7). Bars = 100 nm.

Table 2
Observed spacings and intensities of αFFP diffraction patterns

	Observed			Calculated, hexagonal packing	
	Spacing (*d*; nm)	Intensity	Form of the reflection[a]	Spacing (*d*, nm)	Index
Set I	2.45 ± 0.05	middle	ring	2.44[b]	10
	1.42 ± 0.03	middle	ring	1.41[b]	11
	1.22 ± 0.02	middle	ring	1.22[b]	20
	0.52 ± 0.01	very weak	arc, m, diffuse	α-helical, m	
Set II	2.32 ± 0.05	very strong	ring	2.30[c]	10
	2.13 ± 0.05	very strong	arc, e	2.14[d]	10
	1.33 ± 0.03	middle	ring	1.33[c]	11
	1.24 ± 0.02	strong	arc, e	1.24[d]	11
	1.135 ± 0.02	middle	ring	1.15[c]	20
	1.07 ± 0.02	middle	arc, e	1.07[d]	20
	0.87 ± 0.02	weak	diffuse ring	0.83[c] (0.87[e])	21
	0.83 ± 0.02	middle	diffuse arc, n-e	0.77[d] (0.81[e])	21
	0.51 ± 0.01	very weak	arc, m	α-helical, m	

[a]m, meridional; e, equatorial; n-e, near-equatorial. Equator coincides with axis of the capillary.
[b]$a = 2.82$ nm.
[c]$a = 2.652$ nm.
[d]$a = 2.470$ nm, oriented portion.
[e]Calculated assuming coherently scattering bunches with a limited number (here 19) of hexagonally packed fibrils.

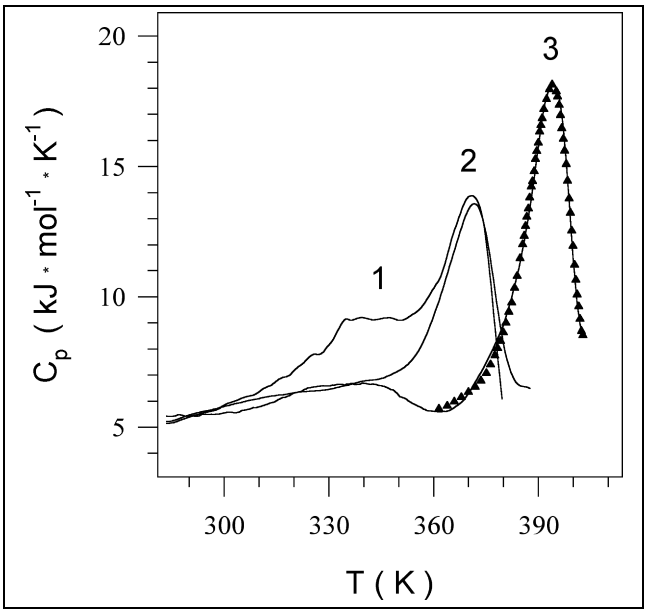

Fig. 4. Temperature dependence of partial molar heat capacity of αFFP in 10 mM sodium phosphate buffer, pH 2.5 at different concentrations of DMSO. 75% DMSO, first (1) and second (2) heatings; (3) 60% DMSO, first heating. Peptide concentration was 1.2 mg/ml. Triangles show a calculated curve which has the best fit of the experimental functions.

pletely which evidences the restoration of the fibril structure at cooling. Furthermore, at a lower temperature the presence of an additional small absorption peak that disappears upon repeated cooling might be connected with the melting of non-equilibrium residual structures. The observed effect of the heating rate on the position of the peak also supports the non-equilibrium character of the melting process. As demonstrated previously, slowdown of the denaturation kinetics often takes place at the addition of organic solvents [22] and, in particular, of DMSO [20]. Thus, most probably, the presence of DMSO, rather than the intrinsic features of the fibrils, causes the slow kinetics of the denaturation.

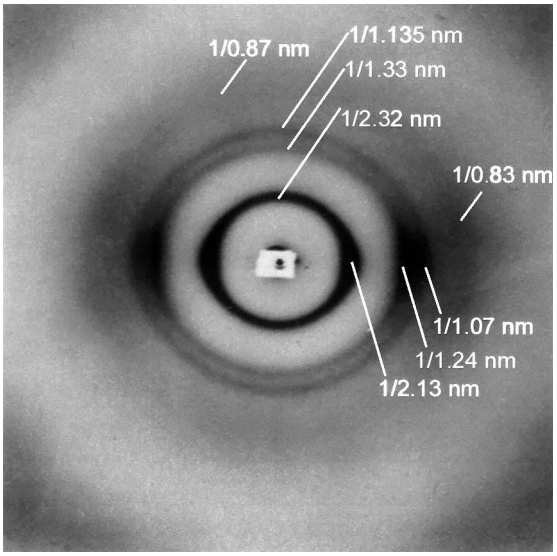

Fig. 5. X-ray diffraction diagram taken from the dry specimen of αFFP.

This cooperative melting of the fibrils and their uniform shape, as seen in the electron microscope, suggest a defined molecular structure. The X-ray diffraction analysis revealed a substantial crystalline component in the αFFP specimen (set I of Table 2). In accordance with this result, the fibrils have a hexagonal packing with 2.82 ± 0.05 nm distance between the adjacent fibrils (Table 2). This is in agreement with the closest distance between the five-stranded coiled coils observed in the crystal of the cartilage oligomeric matrix protein assembly domain [8]. The X-ray diagram also has a 1/0.51 nm^{-1} reflection which is characteristic of the α-helical coiled coils [23]. Subsequent drying of the specimen led to its partial orientation at the areas of the capillary meniscus. Indeed, the X-ray diagram of the dry specimen, in addition to the ring reflections, had several equatorial and one meridional peaks (Fig. 5 and set II of Table 2). The oriented portion of the fibrils gives a 1/0.51 nm^{-1} meridional reflection and this proves that α-helices are oriented along the fibrils. The oriented fibrils are almost perpendicular to the capillary axis and, probably, belong to the texture of the capillary meniscus. The near-equatorial and near-meridional locations of 1/0.83 nm^{-1} and 1/0.51 nm^{-1} reflections, correspondingly, suggest a slight ($\pm 15°$) tilt of fibrils relative to this perpendicular direction.

The interfibrillar distance in the 'dry' oriented portion of the specimen drops to 2.47 ± 0.05 nm (or to 2.65 ± 0.05 nm assuming coherent scattering bunches with a limited number of hexagonally packed fibrils [24], Table 2) and from this value the drying did not further affect it. It allows us to suggest that this minimal value is close to the van der Waals diameter of the fibrils. Molecular modeling showed that the estimated diameter might fit the size of both four- and five-stranded ropes. For example, our calculation of packing energy between modeled five-stranded coiled coils shows that these coiled coils can come as close as 2.6 nm to each other without generating the sterical tension.

3. Discussion

The experimental data show that αFFP is able to self-assemble into uniform soluble fibrils with a diameter of 2.5 nm and α-helices oriented along the fibrils. Although there are a number of known β-structural fibrils with defined diameter formed by short peptides [25,26], αFFP is the first example of an α-helical peptide with such fibril-forming property. The fact that the designed sequence, chosen among more than a million possible coiled coil heptad combinations, self-assembles in a expected fibril arrangement has demonstrated the credibility of our conception of

design. At the same time, the fact that the fibrillogenesis occurs below pH 6, while the peptide was designed to form fibrils at neutral pH, suggests that the importance of **f–g′** salt bridges in the fibril formation was overestimated. Probably, the main factors of fibrillogenesis are the length of the coiled coil fragment and widening of its hydrophobic cluster by placement of alanine in position **e**, as well as hydrogen bonding of glutamines in positions **b** and **c**. Favorable **f–g′** interactions between arginines and glutamic acids cannot be completely ruled out, because these residues can form hydrogen bonds even at acid pH.

The anticipated five-stranded fibril (Fig. 1) is the most suitable model to explain the obtained set of the experimental data: the fibril diameter, completely α-helical peptide conformation and orientation of the helices along the fibril. The 34-residue α-helices of αFFP perfectly fit a parallel five-stranded fibril with one-heptad axial shift of the adjacent α-helices (Fig. 1b). Molecular modeling suggests a slightly thinner diameter of the fibrils, compared with the known pentamers [8], due to the location of smaller Ala residues in the **e** positions of the design peptide. This is in agreement with the 2.47 nm (or 2.65 nm) diameter of the fibrils estimated by X-ray analysis (Table 2). The alternative of the five-stranded coiled coil is a parallel four-stranded fibril with a 27-residue α-helix (79%) and the remaining seven residues of αFFP bulged from the fibril in non-helical conformation. Both the unfolding of one heptad repeat and the lower α-helicity compared to more than 95% of the experimental one make this model less probable, but it cannot be completely ruled out. However plausible a structural model of the five-stranded rope may be, it needs additional experimental support. Although the elongated shape of the fibril hampers the prospects for X-ray crystallography, further investigation hopefully will lead to the solution of its detail structure.

The discovery of a short peptide, able to self-assemble into α-helical fibrils, is a first step to the future engineering of the coiled coils with new desirable properties. We synthesized peptides with five to eight additional residues of non-coiled coil sequence at the N-terminus. The CD and electron microscopy studies show that these peptides have properties analogous to those of original αFFP (Fig. 2b). The fact that αFFP with additional non-coiled coil fragment still forms the fibril suggests that addition of a variety of biologically active ligands will not disrupt the fibril formation. In this case, hundreds of copies of the ligand may protrude from the fibril and impart high multivalency to the complex. As an example, Fig. 1c shows an arrangement of the ligands in the five-stranded fibril model. This property of our peptide can be widely used in medical treatments and biotechnological processes where a higher efficiency can be achieved by associating a larger number of functional subunits into one complex [7,27,28]. Attachment of groups taking part in the electron or any other transfer can also produce a 'peptide wire' with numerous transmitter abilities. Remarkably, at high concentration, upon drying, the fibrils form a hydrogel. The pH-modulated behavior of αFFP is especially useful to create stimulus-sensitive hydrogels, which may have applications requiring encapsulation or controlled release of molecular and cellular species [29,30]. In relation with the encapsulation, knowledge about the structure of the spherical aggregates formed by αFFP at neutral pH is also very important. Unfortunately, the conventional experimental methods can provide little information about their molecular structure. CD spectroscopy data suggest that most of the peptide residues are in the α-helical conformation (Fig. 2). The spheres can be formed by laterally packed α-helices. If so, the apolar surfaces of the α-helices, most probably, are in contact with each other, while the charged and polar residues can form interhelical hydrogen and ionic bonds. However, this hypothesis requires further experimental examinations.

It should also be mentioned that the self-propagating behavior of αFFP resembles formation of amyloid- and prion-like fibrils with one difference: the conformations of the known amyloid deposits are predominantly β-structural [25,26,31] while the fibrils described here are α-helical. The finding of αFFP points to a possibility of human diseases which can be associated with the deposition of α-helical, not only β-structural, fibrils.

4. Significance

Comparative analysis of the known α-helical coiled coil structures allowed us to formulate a hypothesis about factors which may govern the formation of long α-helical fibrils from short peptides. To test this hypothesis we designed and synthesized a 34-residue peptide which was predicted to form a five-stranded coiled coil fibril with α-helices staggered along the axis. Indeed, the experimental data revealed that the peptide spontaneously forms α-helical fibrils with 2.5 nm diameter at slightly acid pH. The observed diameter of the fibrils, α-helical conformation of the peptide and the orientation of α-helices along the fibril axis agree well with the anticipated five-stranded arrangement. To our knowledge, this is the first α-helical peptide with such fibril-forming potential. The experimental analysis also shows that the fibrils can be easily transformed into spherical aggregates at neutral pH and this transformation is completely reversible.

The unique fibril-forming ability and stimulus-sensitive behavior of the designed αFFP open new opportunities for a number of applications in biotechnology and medicine. A coiled coil with such a large number of subunits is especially promising as a scaffold for the construction of multivalent fusion proteins. Indeed, it was shown that αFFP which was fused with a non-coiled coil fragment still forms the fibril. This suggests that fusion of αFFP with active ligands will not disrupt fibril formation. In this case, a large number of copies of the ligand may

protrude from the fibril and impart high multivalency to the complex. This property of αFFP can be widely used in medical treatments and biotechnological processes where a higher efficiency can be achieved by associating a larger number of functional subunits into one complex [7,27,28].

The pH-modulated behavior of αFFP can be used to create stimulus-sensitive hydrogels, which may have applications requiring encapsulation and controlled release of molecules or cells.

5. Materials and methods

5.1. Peptide synthesis

Peptides were synthesized on a peptide synthesizer (Applied Biosystems 431A) and purified by a combination of size exclusion liquid chromatography (Sephadex G25 column 50×2 cm using 50% acetic acid/H_2O as mobile phase) and RP-HPLC (SS250×1/2 in/10 Nucleosil 300-7 C18 using a 0–45% CH_3CN gradient in 0.1% TFA/H_2O in 30 min with a flow rate of 3 ml/min). The purity of peptides was analyzed by RP-HPLC (C18 analytical column) and mass spectroscopy. Peptide concentration was measured by the nitrogen determination method [32].

5.2. CD measurements

CD spectra were obtained on a Jasco-600 spectropolarimeter (Japan Spectroscopic Co.) equipped with a temperature-controlled holder in 0.185 mm thick cells at a peptide concentration of 0.3–0.5 mg/ml. The molar ellipticity was calculated from the equation

$$[\theta] = [\theta]_{obs} M_{res}/(10cL)$$

where $[\theta]_{obs}$ is the ellipticity measured in degrees at wavelength λ, M_{res} is the mean residue molecular weight of peptide, c is the peptide concentration (g/l) and L is the optical path length of the cell (mm). The percentage of α-helicity has been calculated as described in [33].

5.3. Sedimentation–diffusion experiments

Sedimentation–diffusion experiments were performed in 0.1 M NaCl, 10 mM Na-phosphate, pH 2.8 buffer solution using a Beckman Model E analytical ultracentrifuge with the Schliren optical system. The sedimentation coefficient was evaluated at a speed of 42 040 rpm by standard procedure [34]. The diffusion experiments were carried out at the same conditions at a speed of 12 590 rpm.

5.4. Electron microscopy

Samples were studied with a JEOL JEM100B electron microscope. The magnification for each micrograph was calibrated using grating replicas (2160 lines/mm). For staining of sample suspensions the water solution of 2% uranylacetate was used. 5–10 μl of this sample was placed on a grid with Pioloform film. The grids on the copper holder were transferred through the airlock into a vacuum chamber of a freeze-etch apparatus [35]. The angle between the flow of evaporated Pt particles and the grid surface was about 5°. All operations were carried out in vacuum of $2–4\times10^{-6}$ Torr and at a temperature of 173 K. During Pt evaporation the object holder with the grid was rotated. The thickness of the replica was ~2 nm.

5.5. Calorimetric measurements

Calorimetric measurements were made on a precision scanning microcalorimeter SCAL-1 (Scal Co., Russia) with 0.33 ml glass cells at a scanning rate of 1 K/min and under 2.5 atm pressure. The peptide concentrations ranged from 0.5 to 2.0 mg/ml in 10 mM sodium phosphate buffer and pH 2.5. The data were analyzed after scan rate normalization and the baseline subtraction was done as described [36]. The fitting of the experimental curves with theoretical ones was done using the relationship for an irreversible one-stage process described in [37]:

$$c_{p,exc} = e c_p^{max} \exp\left[\frac{\Delta E_{uf}(T-T_m)}{RT_m^2}\right] \exp\left\{\exp\left[\frac{\Delta E_{uf}(T-T_m)}{RT_m^2}\right]\right\}$$

where T_m is the apparent temperature of denaturation, ΔE_{uf} is the activation energy of unfolding, c_p^{max} is the excessive heat capacity at the maximum of the trace, e stands for the natural logarithm base, T is the absolute temperature, R is the gas constant. Van't Hoff enthalpy was calculated as [36]:

$$\Delta H_{eff} = \frac{4RT_m^2}{\Delta H_{cal}} c_p^{max},$$

where ΔH_{cal} is the calorimetric enthalpy.

5.6. X-ray fiber diffraction

The gel-like specimen of fibrils formed at pH 2.8 was packed into the X-ray quartz capillary with a diameter of 1 mm and wall thickness 0.1 mm. The X-ray data were collected using the Searle X-ray camera (UK) completed with Elliott toroidal mirror focussing optics mounted on GX-20 rotating anode X-ray generator (UK) with nickel-filtered copper radiation, operated at 40 kV and 50 mA. Patterns were recorded on flat direct-exposure X-ray film (Retina, Germany), during exposure times of 3–18 h. The specimen-to-film distance ranged from 40 to 155 mm.

Acknowledgements

We thank K.S. Vassilenko for the assistance with CD measurements, V. Brossard for the peptide purification and Drs. U. Blum-Tirouvanziam, A.V. Finkelstein and A.C. Steven for reading the manuscript and criticism. This work was funded in part by the Swiss National Science Foundation (Grant 7SUPJ048578) and Russian Foundation for Basic Research (Grant 98-04-50029).

References

[1] J.W. Bryson, S.F. Betz, H.S. Lu, D.J. Suich, H.X. Zhou, K.T. O'Neil, W.F. DeGrado, Protein design: a hierarchic approach, Science 270 (1995) 935–941.

[2] P.B. Harbury, J.J. Plecs, B. Tidor, T. Alber, P.S. Kim, High-resolu-

tion protein design with backbone freedom, Science 282 (1998) 1462–1467.
[3] R.S. Hodges, Boehringer Mannheim award lecture 1995, *De novo* design of alpha-helical proteins: basic research to medical applications, Biochem. Cell. Biol. 74 (1996) 133–154.
[4] A. Lupas, Predicting coiled-coil regions in proteins, Curr. Opin. Struct. Biol. 7 (1997) 388–393.
[5] M.J. Pandya, G.M. Spooner, M. Sunde, J.R. Thorpe, A. Rodger, D.N. Woolfson, Sticky-end assembly of a designed peptide fiber provides insight into protein fibrillogenesis, Biochemistry 39 (2000) 398728–398734.
[6] N.L. Ogihara, G. Ghirlanda, J.W. Bryson, M. Gingery, W.F. DeGrado, D. Eisenberg, Design of three-dimensional domain-swapped dimers and fibrous oligomers, Proc. Natl. Acad. Sci. USA 98 (2001) 1404–1409.
[7] A.V. Terskikh, J.M. LeDoussal, R. Crameri, I. Fisch, J.P. Mach, A.V. Kajava, 'Peptabody': a new type of high avidity binding protein, Proc. Natl. Acad. Sci. USA 94 (1997) 1663–1668.
[8] V.N. Malashkevich, R.A. Kammerer, V.P. Efimov, T. Schulthess, J. Engel, The crystal structure of a five-stranded coiled coil in COMP: a prototype ion channel?, Science 274 (1996) 761–765.
[9] H.E. Dayring, A. Tramonato, S.R. Sprang, R.J. Fletterick, Interactive program for visualization and modeling of proteins, nucleic acids and small molecules, J. Mol. Graph. 4 (1986) 82–87.
[10] R. Lutgring, J. Chmielewski, General strategy for covalently stabilizing helical bundles – a novel 5-helix bundle, J. Am. Chem. Soc. 116 (1994) 6451–6452.
[11] A.V. Kajava, Modeling of a five-stranded coiled coil structure for the assembly domain of the cartilage oligomeric matrix protein, Proteins 24 (1995) 218–226.
[12] E.K. O'Shea, J.D. Klemm, P.S. Kim, T. Alber, X-ray structure of the GCN4 leucine zipper, a two-stranded, parallel coiled coil, Science 254 (1994) 539–544.
[13] P.B. Harbury, T. Zhang, P.S. Kim, T. Alber, A switch between two-, three-, and four-stranded coiled coils in GCN4 leucine zipper mutants, Science 262 (1993) 1401–1407.
[14] P.B. Harbury, P.S. Kim, T. Alber, Crystal structure of an isoleucine-zipper trimer, Nature 371 (1994) 80–83.
[15] S.A. Potekhin, V.N. Medvedkin, I.A. Kashparov, S.Yu. Venyaminov, Synthesis and properties of the peptide corresponding to the mutant form of the leucine zipper of the transcriptional activator GCN4 from yeast, Protein Eng. 7 (1994) 1097–1101.
[16] S. Alberti, S. Oehler, B. von Wilcken-Bergmann, B. Muller-Hill, Genetic analysis of the leucine heptad repeats of Lac repressor: evidence for a 4-helical bundle, EMBO J. 12 (1993) 3227–3236.
[17] D. Krylov, I. Mikhailenko, C. Vinson, A thermodynamic scale for leucine zipper stability and dimerization specificity: e and g interhelical interactions, EMBO J. 13 (1994) 2849–2861.
[18] O.D. Monera, N.E. Zhou, C.M. Kay, R.S. Hodges, Comparison of antiparallel and parallel two-stranded α-helical coiled coil. Design, synthesis and characterization, J. Biol. Chem. 268 (1993) 19218–19227.
[19] N.E. Zhou, C.M. Kay, R.S. Hodges, Synthetic model proteins the relative contributions of leucine residues at the nonequivalent positions of the 3–4 hydrophobic repeat to the stability of the two-stranded α-helical coiled coil, Biochemistry 31 (1992) 5739–5746.
[20] E.L. Kovrigin, S.A. Potekhin, Microcalorimetric study of the effect of dimethylsulfoxide on the heat denaturation of lysozyme, Biofizika 41 (1996) 1201–1206.
[21] S.A. Potekhin, E.L. Kovrigin, Kinetic effect on heat denaturation and renaturation of biopolymers, Biofizika 43 (1998) 223–232.
[22] K. Griebenow, A.M. Klibanov, On protein denaturation in aqueous-organic mixtures but note in pure organic solvents, J. Am. Chem. Soc. 118 (1996) 1170–1175.
[23] F.H.C. Crick, The Fourier transform of a coiled-coil, Acta Crystallogr. 6 (1953) 685–689.
[24] R.E. Burge, Equatorial X-ray diffraction by fibrous proteins: Short-range order in collagen, feather keratin and F-actin, J. Mol. Biol. 7 (1963) 213–224.
[25] F.E. Cohen, S.B. Prusiner, Pathologic conformations of prion proteins, Annu. Rev. Biochem. 67 (1998) 793–819.
[26] K.L. Taylor, N. Cheng, R.W. Williams, A.C. Steven, R.B. Wickner, Prion domain initiation of amyloid formation in vitro from native Ure2p, Science 283 (1999) 1339–1343.
[27] P.K. Sorger, C.M. Nelson, Trimerization of a yeast transcriptional activator via a coiled coil motif, Cell 59 (1989) 807–813.
[28] P. Pack, A. Pluckthun, Miniantibodies use of amphipathic helices to produce functional, flexibility linked dimeric Fv fragments with high avidity in *Escherichia coli*, Biochemistry 31 (1992) 1579–1584.
[29] W.A. Petka, J.L. Harden, K.P. McGrath, D. Wirtz, D.A. Tirrell, Reversible hydrogels from self-assembling artificial proteins, Science 281 (1998) 389–392.
[30] C. Wang, R.J. Stewart, J. Kopecek, Hybrid hydrogels assembled from synthetic polymers and coiled-coil protein domains, Nature 397 (1999) 417–420.
[31] M. Sunde, C. Blake, The structure of amyloid fibrils by electron microscopy and X-ray diffraction, Adv. Protein Chem. 50 (1997) 123–159.
[32] L. Jaenicke, A rapid micromethod for the determination of nitrogen and phosphate in biological material, Anal. Biochem. 61 (1974) 623–627.
[33] Y.H. Chen, J.T. Yang, K.H. Chau, Determination of the helix and beta form of proteins in aqueous solution by circular dichroism, Biochemistry 13 (1974) 3350–3359.
[34] T.J. Bowen, An Introduction to Ultracentrifugation. Wiley-Interscience, London, 1971.
[35] V.I. Popov, A.A. Nikonov, N.K. Agafonova, E.E. Fesenko, Surface ultrastructure of olfactory receptor sense hairs in the silkmoth, *Antheraea pernyi*, J. Microsc. 174 (1994) 39–46.
[36] P.L. Privalov, S.A. Potekhin, Scanning microcalorimetry in studying temperature-induced changes in proteins, Methods Enzymol. 131 (1986) 1–51.
[37] F. Conejro-Lara, J.M. Sanchez-Ruiz, P.L. Mateo, F.J. Burgos, J. Vandrell, F.X. Aviles, Differential scanning calorimetric study of carboxypeptidase B, procarboxypeptidase B and its globular activation domain, Eur. J. Biochem. 200 (1991) 663–670.